

A complex variable boundary element method for solving a steady-state advection-diffusion-reaction equation⁺

Xue Wang and Whye-Teong Ang*
School of Mechanical and Aerospace Engineering
Nanyang Technological University
639798 Singapore

Abstract

An accurate complex variable boundary element method is proposed for the numerical solution of two-dimensional boundary value problems governed by a steady-state advection-diffusion-reaction equation. With the aid of the Cauchy integral formulae, the task of constructing a complex function which gives the solution of the boundary value problem under consideration is reduced to solving a system of linear algebraic equations. The method is applied to solve several specific problems which have exact solutions in closed form and a problem of practical interest in engineering.

Keywords: Complex variable boundary element method; Advection-diffusion-reaction equation; Boundary elements; Numerical method.

* Author for correspondence.
Tel: (65) 6790-5937.
E-mail: mwtang@ntu.edu.sg

+ This is a preprint of the paper published in:
Applied Mathematics and Computation **321** (2018) 731-744.

1 Introduction

Partial differential equations play an important role in the understanding of physical phenomena in engineering science. Thus, many researchers devote their attention to finding and investigating analytical and numerical solutions of problems governed by various differential equations. For example, Ang [2] proposed a dual-reciprocity boundary element solution for the system of partial differential equations in the two-dimensional reaction-diffusion Brusselator system, Dai and Nassar [8] solved approximately the Schrodinger equation in quantum mechanics using a finite difference scheme, Gumel et al. [9] developed an efficient parallel algorithm for the numerical solution of the two-dimensional diffusion equation, and Skote [16] performed a scaling analysis of solutions for velocity profiles in drag reduced turbulent flows over an oscillating wall.

The present paper considers the boundary value problem of solving the partial differential equation

$$\lambda\left(\frac{\partial^2\phi}{\partial x^2} + \frac{\partial^2\phi}{\partial y^2}\right) - u\frac{\partial\phi}{\partial x} - v\frac{\partial\phi}{\partial y} - k\phi = 0 \text{ in } R, \quad (1)$$

subject to the boundary condition

$$f(x, y)\frac{\partial\phi}{\partial n} + g(x, y)\phi = s(x, y) \text{ on } C, \quad (2)$$

where ϕ is the unknown function which depend on x and y which are Cartesian coordinates, λ is a positive constant, u , v and k are constant coefficients, f , g and s are suitably given functions for (x, y) on C such that $[f(x, y)]^2 + [g(x, y)]^2 \neq 0$, R is a two-dimensional bounded region on the Oxy plane, C is the simple closed curve which bounds the region R , $\partial\phi/\partial n = \mathbf{n} \cdot \nabla\phi$ and $\mathbf{n} = [n_x, n_y]$ is the unit normal vector on C pointing away from R .

From a physical standpoint, the partial differential equation (1) describes a two-dimensional advection-diffusion process which involves the steady state transport of the quantity ϕ in the presence of a first order reaction in a homogeneous isotropic region. The constant coefficient λ is the diffusivity, (u, v) is the convective velocity and k is the reaction rate.

Recently, Singh and Tanaka [15] used an exponential variable transformation (introduced by Li and Evans [11]) to convert (1) into a modified Helmholtz equation. The standard boundary element method for the modified Helmholtz equation was then applied to solve numerically the boundary value problem defined by (1) and (2). A brief review of earlier boundary element approaches for solving the boundary value problem may be found in [15].

In the present paper, a different boundary element approach – one based on the Cauchy integral formulae and known as the complex variable boundary element method – is proposed for the numerical solution of (1) subject to (2). The Cauchy integral formulae are used to reduce the boundary value problem to solving a system of linear algebraic equations. The proposed method should offer itself as an interesting and useful alternative to the earlier boundary element techniques for solving two-dimensional steady-state advection-diffusion-reaction problems. To validate the method proposed here, it is applied to solve several problems which have closed form analytical solutions.

Hromadka and Lai [10] were among the earliest researchers to apply the Cauchy integral formula to derive a complex variable boundary element method for solving numerically problems governed by the two-dimensional Laplace equation. Ang and Park [3] proposed a version of the complex variable boundary element method for the numerical solution of a general system

of elliptic partial differential equations in two-dimensional space. Park and Ang [13] extended the work in [3] to include an elliptic partial differential equation with variable coefficients. The approach in [3] and [13] differs from that in [10] in the manner in which the flux boundary conditions are treated. The flux boundary conditions were approximated using a differentiated form of the Cauchy integral formula in [3] and [13]. The same complex variable approach was also independently introduced by Chen and Chen [6] for two-dimensional potential problems with or without degenerate boundaries. For examples of applications of the complex variable boundary element method to various problems in engineering science, one may refer to Barone et al. [4], Barone and Pirrotta [5], Sato [14] and references therein.

2 Complex Formulation

Guided by the analyses in Ang [1] and Clements and Rogers [7], to seek solutions of (1) in terms of complex functions, we write:

$$\phi(x, y) = \operatorname{Re}\left\{\sum_{m=0}^{\infty} h_m(x)\Phi_m(z)\right\}, \quad (3)$$

where $z = x + iy$, $i = \sqrt{-1}$, h_m are functions to be determined, Φ_m are complex functions that are analytic in $R \cup C$ and Re denotes the real part of a complex number.

Substitution of (3) into (1) yields

$$\begin{aligned} \operatorname{Re} \sum_{m=0}^{\infty} ([2\lambda h'_m(x) - (u + iv)h_m(x)]\Phi'_m(z) \\ + [\lambda h''_m(x) - uh'_m(x) - kh_m(x)]\Phi_m(z)) = 0, \end{aligned} \quad (4)$$

where the prime denotes differentiation with respect to the relevant argument.

Now if the functions $\Phi_m(z)$ are required to satisfy the recurrence relation

$$\Phi'_m(z) = m\Phi_{m-1}(z) \text{ for } m = 1, 2, 3, \dots, \quad (5)$$

then from (4) we find that (1) admits non-trivial solutions of the form (3) provided that

$$\begin{aligned} & 2\lambda h'_m(x) - (u + iv)h_m(x) \\ &= \frac{-\lambda h''_{m-1}(x) + uh'_{m-1}(x) + kh_{m-1}(x)}{m} \text{ for } m = 1, 2, 3, \dots, \end{aligned} \quad (6)$$

with $h_0(x) = \exp([u + iv]x/[2\lambda])$.

We can solve (6) as a first order ordinary differential equation for h_m in terms of h_{m-1} . This gives

$$h_m(x) = h_0(x) \int \frac{[-\lambda h''_{m-1}(x) + uh'_{m-1}(x) + kh_{m-1}(x)] dx}{2\lambda m h_0(x)} \text{ for } m = 1, 2, \dots. \quad (7)$$

For convenience, the arbitrary constant arising out of the indefinite integration in (6) can be neglected. Notice that (6) is satisfied by $h_m(x)/h_0(x)$ being a polynomial function of order m . The coefficients of the polynomial function are given by recurrence relations in the Appendix.

Repeated application of the recurrence relation (5) gives

$$\Phi_m(z) = m \int_a^z (z - t)^{m-1} \Phi_0(t) dt \text{ for } m = 1, 2, \dots, \quad (8)$$

where the complex integration from a to z can be taken along any path that lies in $R \cup C$. Thus, (3) can now be rewritten as:

$$\phi(x, y) = \text{Re}\{h_0(x)\Phi_0(z) + \sum_{m=1}^{\infty} mh_m(x) \int_a^z (z - t)^{m-1} \Phi_0(t) dt\}. \quad (9)$$

With (9) together with $h_m(x)$ as known functions, the boundary value problem defined by (1) and (2) can now be reformulated as a problem which

requires us to construct a complex function Φ_0 which is analytic in $R \cup C$ and such that

$$\begin{aligned}
& f(x, y) \operatorname{Re}\{(n_x + in_y)[h_0(x)\Phi'_0(z) + h_1(x)\Phi_0(z) \\
& + \sum_{m=2}^{\infty} m(m-1)h_m(x) \int_a^z (z-t)^{m-2}\Phi_0(t)dt] \\
& + n_x[h'_0(x)\Phi_0(z) + \sum_{m=1}^{\infty} mh'_m(x) \int_a^z (z-t)^{m-1}\Phi_0(t)dt] \\
& + g(x, y)[h_0(x)\Phi_0(z) + \sum_{m=1}^{\infty} mh_m(x) \int_a^z (z-t)^{m-1}\Phi_0(t)dt]\} \\
& = s(x, y) \text{ for } (x, y) \in C.
\end{aligned} \tag{10}$$

3 Complex Variable Boundary Element Method

The required function $\Phi_0(z)$ for the solution of the boundary value problem under consideration is constructed by using the Cauchy integral formula

$$2\pi i\Phi_0(z_0) = \int_C \frac{\Phi_0(z)dz}{z - z_0} \text{ for } z_0 \in R, \tag{11}$$

and

$$\left. \begin{aligned}
\pi i\Phi_0(z_0) &= \mathcal{C} \int_C \frac{\Phi_0(z)dz}{(z - z_0)} \\
\pi i\Phi'_0(z_0) &= \mathcal{H} \int_C \frac{\Phi_0(z)dz}{(z - z_0)^2}
\end{aligned} \right\} \text{ for } z_0 \text{ on a smooth part of } C, \tag{12}$$

where the contour C is assigned an anticlockwise direction and \mathcal{C} and \mathcal{H} imply that the complex integral over C are to be interpreted in the Cauchy principal and Hadamard finite-part respectively as explained in detail in Linkov and Mogilevskaya [12].

To discretize the curve boundary C , M well-spaced out points $(x^{(1)}, y^{(1)})$, $(x^{(2)}, y^{(2)})$, \dots , $(x^{(M-1)}, y^{(M-1)})$ and $(x^{(M)}, y^{(M)})$ are placed on it in an anti-clockwise order. Denote the directed straight line segment from $(x^{(k)}, y^{(k)})$ to $(x^{(k+1)}, y^{(k+1)})$ by $C^{(k)}$ ($k = 1, 2, \dots, M$). [We define $(x^{(M+1)}, y^{(M+1)}) = (x^{(1)}, y^{(1)})$.] We make the approximation:

$$C \simeq C^{(1)} \cup C^{(2)} \cup \dots \cup C^{(M-1)} \cup C^{(M)}, \quad (13)$$

such that (11) may be written as

$$2\pi i \Phi_0(z_0) = \sum_{m=1}^M \int_{C^{(m)}} \frac{\Phi_0(z) dz}{z - z_0} \text{ for } z_0 \in R. \quad (14)$$

The function $\Phi_0(z)$ over the line segment $C^{(m)}$ is approximated as a linear function of z by

$$\Phi_0(z) \simeq \phi^{(m)} + \phi^{(m+M)} z \text{ for } z \text{ on } C^{(m)}, \quad (15)$$

where $\phi^{(m)}$ and $\phi^{(m+M)}$ are complex constants to be determined.

If we substitute (15) into (14) and let z_0 approach the point $c^{(k)} = (3z^{(k)} + z^{(k+1)})/4$ on the k -th element $C^{(k)}$, where $z^{(m)} = x^{(m)} + iy^{(m)}$ for $m = 1, 2, \dots$, we find that the real parts of the resulting equations are given by

$$\begin{aligned} & -\pi(\nu^{(k)} + \eta^{(k)}\mu^{(k+M)} + \xi^{(k)}\nu^{(k+M)}) \\ & = \sum_{m=1}^M \{ \gamma(\widehat{z}^{(m)}, z^{(m+1)}, c^{(k)}) [\mu^{(m)} + \xi^{(k)}\mu^{(m+M)} - \eta^{(k)}\nu^{(m+M)}] \\ & - \theta(\widehat{z}^{(m)}, z^{(m+1)}, c^{(k)}) [\nu^{(m)} + \eta^{(k)}\mu^{(m+M)} + \xi^{(k)}\nu^{(m+M)}] \\ & + (x^{(m+1)} - x^{(m)})\mu^{(m+M)} - (y^{(m+1)} - y^{(m)})\nu^{(m+M)} \} \\ & \text{for } k = 1, 2, \dots, M, \end{aligned} \quad (16)$$

where $\mu^{(p)}$ and $\nu^{(p)}$ are respectively the real and imaginary parts of $\phi^{(p)}$ ($p = 1, 2, \dots, 2M$), $\xi^{(k)}$ and $\eta^{(k)}$ are the real and imaginary parts of $c^{(k)}$ respectively and

$$\begin{aligned}\tilde{z}^{(m)} &= \begin{cases} \frac{1}{2}(z^{(m)} + z^{(m+1)}) & \text{if } m = k, \\ z^{(m)} & \text{if } m \neq k, \end{cases} \\ \gamma(a, b, c) &= \ln |b - c| - \ln |a - c|, \\ \theta(a, b, c) &= \begin{cases} \Theta(a, b, c) & \text{if } \Theta(a, b, c) \in (-\pi, \pi], \\ \Theta(a, b, c) + 2\pi & \text{if } \Theta(a, b, c) \in [-2\pi, -\pi], \\ \Theta(a, b, c) - 2\pi & \text{if } \Theta(a, b, c) \in (\pi, 2\pi], \end{cases} \\ \Theta(a, b, c) &= \text{Arg}(b - c) - \text{Arg}(a - c), \end{aligned} \quad (17)$$

where $\text{Arg}(z)$ denotes the principal argument of the complex number z . If the solution domain is convex in shape, $\theta(a, b, c)$ can be calculated more directly from

$$\theta(a, b, c) = \cos^{-1}\left(\frac{|b - c|^2 + |a - c|^2 - |b - a|^2}{2|b - c||a - c|}\right). \quad (18)$$

Similarly, by substituting (15) into (14), letting z_0 approach $c^{(k+M)} = (z^{(k)} + 3z^{(k+1)})/4$ on $C^{(k)}$ and taking the real part of the resulting equations, we obtain

$$\begin{aligned} & -\pi(\nu^{(k)} + \eta^{(k+M)}\mu^{(k+M)} + \xi^{(k+M)}\nu^{(k+M)}) \\ &= \sum_{m=1}^M \{ \gamma(z^{(m)}, \tilde{z}^{(m)}, c^{(k+M)})[\mu^{(m)} + \xi^{(k+M)}\mu^{(m+M)} - \eta^{(k+M)}\nu^{(m+M)}] \\ & - \theta(z^{(m)}, \tilde{z}^{(m)}, c^{(k+M)})[\nu^{(m)} + \eta^{(k+M)}\mu^{(m+M)} + \xi^{(k+M)}\nu^{(m+M)}] \\ & + (x^{(m+1)} - x^{(m)})\mu^{(m+M)} - (y^{(m+1)} - y^{(m)})\nu^{(m+M)} \} \\ & \text{for } k = 1, 2, \dots, M, \end{aligned} \quad (19)$$

where $\xi^{(k+M)}$ and $\eta^{(k+M)}$ are respectively the real and imaginary parts of $c^{(k+M)}$ and

$$\tilde{z}^{(m)} = \begin{cases} \frac{1}{2}(z^{(m)} + z^{(m+1)}) & \text{if } m = k, \\ z^{(m+1)} & \text{if } m \neq k. \end{cases} \quad (20)$$

Note that (16) and (19) give a system of $2M$ linear algebraic equations in $4M$ unknowns $\mu^{(p)}$ and $\nu^{(p)}$ ($p = 1, 2, \dots, 2M$). Another $2M$ linear algebraic equations are needed to complete the formulation. They are derived from the boundary condition in (10) as follows.

Taking (x, y) in (10) to be given in turn by $(\xi^{(p)}, \eta^{(p)})$ for $p = 1, 2, \dots, M$, we find the boundary condition may be approximated by

$$\begin{aligned}
& f(\xi^{(p)}, \eta^{(p)}) \left\{ \sum_{n=1}^M (T^{(1pn)} [\mu^{(n)} + \xi^{(p)} \mu^{(n+M)} - \eta^{(p)} \nu^{(n+M)}] \right. \\
& - U^{(1pn)} [\nu^{(n)} + \eta^{(p)} \mu^{(n+M)} + \xi^{(p)} \nu^{(n+M)}] \\
& + V^{(1pn)} \mu^{(n+M)} - W^{(1pn)} \nu^{(n+M)}) \\
& + A^{(1p)} [\mu^{(p)} + \xi^{(p)} \mu^{(p+M)} - \eta^{(p)} \nu^{(p+M)}] \\
& - B^{(1p)} [\nu^{(p)} + \eta^{(p)} \mu^{(p+M)} + \xi^{(p)} \nu^{(p+M)}] \\
& + \sum_{r=1}^p [I^{(1pr)} (\mu^{(r)} + \xi^{(p)} \mu^{(r+M)} - \eta^{(p)} \nu^{(r+M)}) - K^{(1pr)} \mu^{(r+M)} \\
& - J^{(1pr)} (\nu^{(r)} + \eta^{(p)} \mu^{(r+M)} + \xi^{(p)} \nu^{(r+M)}) + L^{(1pr)} \nu^{(r+M)}] \left. \right\} \\
& + g(\xi^{(p)}, \eta^{(p)}) \left\{ \operatorname{Re}(h_0(\xi^{(p)})) [\mu^{(p)} + \xi^{(p)} \mu^{(p+M)} - \eta^{(p)} \nu^{(p+M)}] \right. \\
& - \operatorname{Im}(h_0(\xi^{(p)})) [\nu^{(p)} + \eta^{(p)} \mu^{(p+M)} + \xi^{(p)} \nu^{(p+M)}] \\
& + \sum_{r=1}^p [P^{(1pr)} (\mu^{(r)} + \xi^{(p)} \mu^{(r+M)} - \eta^{(p)} \nu^{(r+M)}) - R^{(1pr)} \mu^{(r+M)} \\
& - Q^{(1pr)} (\nu^{(r)} + \eta^{(p)} \mu^{(r+M)} + \xi^{(p)} \nu^{(r+M)}) + S^{(1pr)} \nu^{(r+M)}] \left. \right\} \\
& = s(\xi^{(p)}, \eta^{(p)}) \text{ for } p = 1, 2, \dots, M, \tag{21}
\end{aligned}$$

where $A^{(1p)}$, $B^{(1p)}$, $T^{(1pn)}$, $U^{(1pn)}$, $V^{(1pn)}$ and $W^{(1pn)}$ are real numbers given

by

$$\begin{aligned}
A^{(1p)} + iB^{(1p)} &= (n_x^{(p)} + in_y^{(p)})h_1(\xi^{(p)}) + n_x^{(p)}h_0'(\xi^{(p)}) \\
T^{(1pn)} + iU^{(1pn)} &= \frac{(n_x^{(p)} + in_y^{(p)})h_0(\xi^{(p)})}{\pi i} \left[-\frac{1}{z^{(n+1)} - c^{(p)}} + \frac{1}{z^{(n)} - c^{(p)}} \right], \\
V^{(1pn)} + iW^{(1pn)} &= \frac{(n_x^{(p)} + in_y^{(p)})h_0(\xi^{(p)})}{\pi i} [\gamma(\widehat{z}^{(n)}, z^{(n+1)}, c^{(p)}) + i\theta(\widehat{z}^{(n)}, z^{(n+1)}, c^{(p)})],
\end{aligned} \tag{22}$$

$[n_x^{(p)}, n_y^{(p)}]$ is the unit normal vector to $C^{(p)}$ pointing away from R , $P^{(1pr)}$, $Q^{(1pr)}$, $R^{(1pr)}$ and $S^{(1pr)}$ are real numbers defined by

$$\begin{aligned}
P^{(1pr)} + iQ^{(1pr)} &= \sum_{m=1}^{\infty} mh_m(\xi^{(p)})\Omega_m^{(1pr)}, \\
R^{(1pr)} + iS^{(1pr)} &= \sum_{m=1}^{\infty} mh_m(\xi^{(p)})\Omega_{m+1}^{(1pr)},
\end{aligned} \tag{23}$$

$I^{(1pr)}$, $J^{(1pr)}$, $K^{(1pr)}$ and $L^{(1pr)}$ are real numbers defined by

$$\begin{aligned}
&I^{(1pr)} + iJ^{(1pr)} \\
&= \sum_{m=1}^{\infty} [(n_x^{(p)} + in_y^{(p)})(m+1)mh_{m+1}(\xi^{(p)}) + n_x^{(p)}mh_m'(\xi^{(p)})]\Omega_m^{(1pr)}, \\
&K^{(1pr)} + iL^{(1pr)} \\
&= \sum_{m=1}^{\infty} [(n_x^{(p)} + in_y^{(p)})(m+1)mh_{m+1}(\xi^{(p)}) + n_x^{(p)}mh_m'(\xi^{(p)})]\Omega_{m+1}^{(1pr)},
\end{aligned} \tag{24}$$

$\Omega_m^{(1pr)}$ are complex constants defined by

$$\Omega_m^{(1pr)} = (1 - \delta^{(rp)}) \int_{z^{(r)}}^{z^{(r+1)}} [c^{(p)} - t]^{m-1} dt + \delta^{(rp)} \int_{z^{(r)}}^{c^{(r)}} [c^{(p)} - t]^{m-1} dt, \tag{25}$$

with $\delta^{(rp)} = 1$ and $\delta^{(rp)} = 0$ if $r \neq p$.

Similarly, if we take (x, y) in (10) to be given in turn by $(\xi^{(p+M)}, \eta^{(p+M)})$

for $p = 1, 2, \dots, M$, the boundary condition may be approximated by

$$\begin{aligned}
& f(\xi^{(p+M)}, \eta^{(p+M)}) \left\{ \sum_{n=1}^M (T^{(2pn)} [\mu^{(n)} + \xi^{(p+M)} \mu^{(n+M)} - \eta^{(p+M)} \nu^{(n+M)}] \right. \\
& - U^{(2pn)} [\nu^{(n)} + \eta^{(p+M)} \mu^{(n+M)} + \xi^{(p+M)} \nu^{(n+M)}] \\
& + V^{(2pn)} \mu^{(n+M)} - W^{(2pn)} \nu^{(n+M)}) \\
& + A^{(2p)} [\mu^{(p)} + \xi^{(p+M)} \mu^{(p+M)} - \eta^{(p+M)} \nu^{(p+M)}] \\
& - B^{(2p)} [\nu^{(p)} + \eta^{(p+M)} \mu^{(p+M)} + \xi^{(p+M)} \nu^{(p+M)}] \\
& + \sum_{r=1}^p [I^{(2pr)} (\mu^{(r)} + \xi^{(p+M)} \mu^{(r+M)} - \eta^{(p+M)} \nu^{(r+M)}) - K^{(2pr)} \mu^{(r+M)} \\
& - J^{(2pr)} (\nu^{(r)} + \eta^{(p+M)} \mu^{(r+M)} + \xi^{(p+M)} \nu^{(r+M)}) + L^{(2pr)} \nu^{(r+M)}] \Big\} \\
& + g(\xi^{(p+M)}, \eta^{(p+M)}) \left\{ \operatorname{Re}(h_0(\xi^{(p+M)})) [\mu^{(p)} + \xi^{(p+M)} \mu^{(p+M)} - \eta^{(p+M)} \nu^{(p+M)}] \right. \\
& - \operatorname{Im}(h_0(\xi^{(p+M)})) [\nu^{(p)} + \eta^{(p+M)} \mu^{(p+M)} + \xi^{(p+M)} \nu^{(p+M)}] \\
& + \sum_{r=1}^p [P^{(2pr)} (\mu^{(r)} + \xi^{(p+M)} \mu^{(r+M)} - \eta^{(p+M)} \nu^{(r+M)}) - R^{(2pr)} \mu^{(r+M)} \\
& - Q^{(2pr)} (\nu^{(r)} + \eta^{(p+M)} \mu^{(r+M)} + \xi^{(p+M)} \nu^{(r+M)}) + S^{(2pr)} \nu^{(r+M)}] \Big\} \\
& = s(\xi^{(p+M)}, \eta^{(p+M)}) \text{ for } p = 1, 2, \dots, M, \tag{26}
\end{aligned}$$

where $A^{(2p)}$, $B^{(2p)}$, $T^{(2pn)}$, $U^{(2pn)}$, $V^{(2pn)}$ and $W^{(2pn)}$ are real numbers given by

$$\begin{aligned}
A^{(2p)} + iB^{(2p)} &= (n_x^{(p)} + in_y^{(p)}) h_1(\xi^{(p+M)}) + n_x^{(p)} h_0'(\xi^{(p+M)}) \\
T^{(2pn)} + iU^{(2pn)} &= \frac{(n_x^{(p)} + in_y^{(p)}) h_0(\xi^{(p+M)})}{\pi i} \left[-\frac{1}{z^{(n+1)} - c^{(p+M)}} + \frac{1}{z^{(n)} - c^{(p+M)}} \right], \\
V^{(2pn)} + iW^{(2pn)} &= \frac{(n_x^{(p)} + in_y^{(p)}) h_0(\xi^{(p+M)})}{\pi i} [\gamma(z^{(n)}, \tilde{z}^{(n)}, c^{(p+M)}) + i\theta(z^{(n)}, \tilde{z}^{(n)}, c^{(p+M)})], \tag{27}
\end{aligned}$$

$P^{(2pr)}$, $Q^{(2pr)}$, $R^{(2pr)}$ and $S^{(2pr)}$ are real numbers defined by

$$\begin{aligned} P^{(2pr)} + iQ^{(2pr)} &= \sum_{m=1}^{\infty} mh_m(\xi^{(p+M)})\Omega_m^{(2pr)}, \\ R^{(2pr)} + iS^{(2pr)} &= \sum_{m=1}^{\infty} mh_m(\xi^{(p+M)})\Omega_{m+1}^{(2pr)}, \end{aligned} \quad (28)$$

$I^{(2pr)}$, $J^{(2pr)}$, $K^{(2pr)}$ and $L^{(2pr)}$ are real numbers defined by

$$\begin{aligned} &I^{(2pr)} + iJ^{(2pr)} \\ &= \sum_{m=1}^{\infty} [(n_x^{(p)} + in_y^{(p)})(m+1)mh_{m+1}(\xi^{(p+M)}) + n_x^{(p)}mh'_m(\xi^{(p+M)})]\Omega_m^{(2pr)}, \\ &K^{(2pr)} + iL^{(2pr)} \\ &= \sum_{m=1}^{\infty} [(n_x^{(p)} + in_y^{(p)})(m+1)mh_{m+1}(\xi^{(p+M)}) + n_x^{(p)}mh'_m(\xi^{(p+M)})]\Omega_{m+1}^{(2pr)}, \end{aligned} \quad (29)$$

and $\Omega_m^{(2pr)}$ are complex constants defined by

$$\Omega_m^{(2pr)} = (1 - \delta^{(rp)}) \int_{z^{(r)}}^{z^{(r+1)}} [c^{(p+M)} - t]^{m-1} dt + \delta^{(rp)} \int_{z^{(r)}}^{c^{(r+M)}} [c^{(p+M)} - t]^{m-1} dt. \quad (30)$$

Once the $4M$ unknowns $\mu^{(p)}$ and $\nu^{(p)}$ ($p = 1, 2, \dots, 2M$) are obtained by solving the linear algebraic equations (16), (19), (21) and (26), the numerical solutions of ϕ at a point (ξ, η) in the interior of the solution domain may be approximately calculated by using

$$\begin{aligned} \phi(\xi, \eta) &= \text{Re} \left\{ \frac{h_0(\xi)}{2\pi i} \sum_{n=1}^M [\phi^{(n+M)}(z^{(n+1)} - z^{(n)}) \right. \\ &\quad + (\phi^{(n)} + \phi^{(n+M)}(\xi + i\eta))[\gamma(z^{(n)}, z^{(n+1)}, \xi + i\eta) + i\theta(z^{(n)}, z^{(n+1)}, \xi + i\eta)] \\ &\quad + \sum_{m=1}^{\infty} \sum_{n=1}^M \frac{h_m(\xi)}{2\pi i} (\Gamma_m^{(n)}(z^{(n+1)} - z^{(n)}) \\ &\quad \left. + (\Psi_m^{(n)} + \Gamma_m^{(n)}(\xi + i\eta))[\gamma(z^{(n)}, z^{(n+1)}, \xi + i\eta) + i\theta(z^{(n)}, z^{(n+1)}, \xi + i\eta)] \right\}, \end{aligned} \quad (31)$$

where $\Gamma_m^{(n)}$ and $\Psi_m^{(n)}$ are given by

$$\Gamma_m^{(n)} = \frac{\Phi_m^{(n)}(c^{(n+M)}) - \Phi_m^{(n)}(c^{(n)})}{c^{(n+M)} - c^{(n)}},$$

$$\Psi_m^{(n)} = \Phi_m^{(n)}(c^{(n)}) - \frac{\Phi_m^{(n)}(c^{(n+M)}) - \Phi_m^{(n)}(c^{(n)})}{c^{(n+M)} - c^{(n)}} c^{(n)},$$

and

$$\Phi_m^{(n)}(c^{(n)}) = m \sum_{k=1}^n [(\phi^{(k)} + \phi^{(k+M)} c^{(n)}) \Omega_m^{(1nk)} - \phi^{(k+M)} \Omega_{m+1}^{(1nk)}],$$

$$\Phi_m^{(n)}(c^{(n+M)}) = m \sum_{k=1}^n [(\phi^{(k)} + \phi^{(k+M)} c^{(n+M)}) \Omega_m^{(2nk)} - \phi^{(k+M)} \Omega_{m+1}^{(2nk)}].$$

4 Specific problems

The complex variable boundary element method outlined in Section 3 is applied here to solve some specific problems.

Problem 1. The boundary value problem here is to solve the Dirichlet problem governed by

$$\frac{\partial^2 \phi}{\partial x^2} + \frac{\partial^2 \phi}{\partial y^2} - u \frac{\partial \phi}{\partial x} = 0 \text{ for } 0 < x < 1, \ 0 < y < 1, \quad (32)$$

subject to

$$\phi = \begin{cases} 0 & \text{on } y = 0 \\ 0 & \text{on } y = 1 \end{cases} \text{ for } 0 < x < 1,$$

$$\phi = \begin{cases} 0 & \text{on } x = 0 \\ \sin(\pi y) & \text{on } x = 1 \end{cases} \text{ for } 0 < y < 1, \quad (33)$$

The analytical solution of the boundary value problem above is given by

$$\phi(x, y) = \left\{ \exp \left(-x \left(\frac{1}{2} \sqrt{u^2 + 4\pi^2} - \frac{1}{2} u \right) \right) - \exp \left(x \left(\frac{1}{2} u + \frac{1}{2} \sqrt{u^2 + 4\pi^2} \right) \right) \right\}$$

$$\times \frac{\sin(\pi y)}{\exp \left(\frac{1}{2} u - \frac{1}{2} \sqrt{u^2 + 4\pi^2} \right) - \exp \left(\frac{1}{2} u + \frac{1}{2} \sqrt{u^2 + 4\pi^2} \right)}. \quad (34)$$

Table 1. A comparison of the numerical and analytical values of $\phi(x, y)$ for $u = 1$ at selected points in the interior of the square domain.

Point (x, y)	$M_0 = 5$	$M_0 = 10$	$M_0 = 20$	Analytical
	$N_0 = 2$	$N_0 = 4$	$N_0 = 8$	
(0.05, 0.05)	0.0013325	0.0013462	0.0013052	0.0012932
(0.05, 0.35)	0.0075252	0.0073876	0.0073706	0.0073655
(0.05, 0.65)	0.0075319	0.0073877	0.0073707	0.0073655
(0.05, 0.95)	0.0013357	0.0013470	0.0013053	0.0012932
(0.35, 0.05)	0.013338	0.012854	0.012794	0.012775
(0.35, 0.35)	0.073170	0.072881	0.072793	0.072762
(0.35, 0.65)	0.073173	0.072882	0.072793	0.072762
(0.35, 0.95)	0.013334	0.012856	0.012794	0.012775
(0.65, 0.05)	0.042416	0.042636	0.042543	0.042514
(0.65, 0.35)	0.24307	0.24246	0.24223	0.24215
(0.65, 0.65)	0.24306	0.24246	0.24223	0.24215
(0.65, 0.95)	0.042381	0.042638	0.042544	0.042514
(0.95, 0.05)	0.13215	0.12992	0.13003	0.13005
(0.95, 0.35)	0.74281	0.74143	0.74098	0.74074
(0.95, 0.65)	0.74279	0.74143	0.74098	0.74074
(0.95, 0.95)	0.13210	0.12992	0.13003	0.13005
Average % error	1.61%	0.73%	0.17%	—

To apply the complex variable boundary element method to the Dirichlet problem above, each side of the square domain is discretized into M_0 elements of equal length (so that the total number of elements is $4M_0$) and the infinite series in (23), (24), (28), (29) and (31) are truncated by replacing ∞ with a positive integer N_0 . In Table 1, numerical values of ϕ for $u = 1$ obtained using specific values of M_0 and N_0 are compared with the analytical solution at selected points in the interior of the square domain. For given set of M_0 and N_0 , average percentage error of the numerical values of ϕ at the selected interior points is given at the bottom of Table 1.

The numerical values of ϕ in Table 1 are quite accurate even for a crude discretization of the boundary ($M_0 = 5$) and a low number of terms in the truncated series ($N_0 = 2$). It is obvious that the average percentage error is significantly reduced when the number of boundary elements and the number of terms are doubled. The average percentage error for $(M_0, N_0) = (20, 8)$ is about ten times smaller than that for $(M_0, N_0) = (5, 2)$.

To achieve a certain level of accuracy in the numerical solution, it may be necessary to use a larger number of terms in the truncated series (that is, larger value of N_0) if the coefficient u in the partial differential equation in (32) has a larger magnitude. For $u = 1$, the average percentage error of the solutions at the 16 points in Table 1 obtained by using $(M_0, N_0) = (10, 4)$ is 0.73%. To achieve approximately the same average percentage error in the numerical values of ϕ for $u = 10$ with $M_0 = 10$ (still), the value of N_0 has to be increased to 16.

Problem 2. Take the governing partial differential equation to be

$$\frac{\partial^2 \phi}{\partial x^2} + \frac{\partial^2 \phi}{\partial y^2} - \frac{\partial \phi}{\partial x} - v \frac{\partial \phi}{\partial y} = 0, \quad (35)$$

and the solution domain to be the triangular region bounded by $x = 0$, $y = 0$ and $y = 1 - x$, that is, the region inside the triangle with vertices $(0, 0)$, $(1, 0)$ and $(0, 1)$.

A particular solution of (35) is

$$\phi(x, y) = v^2 x^2 + y^2 + 2(v^2 + 1)x - 2vxy. \quad (36)$$

We use (36) to generate boundary data on the sides of the triangular domain. Specifically, ϕ is specified on the sides where $x = 0$ and $y = 0$, and $\partial\phi/\partial n$ on the straight line between the vertices $(1, 0)$ and $(0, 1)$. The complex

variable boundary method is then applied to solve numerically (35) subject to the boundary data generated for selected values of v .

For the complex variable boundary element method, we discretize the sides where $x = 0$ and $y = 0$ into $2M_0$ elements, each of length $1/M_0$, and the side where $y = 1 - x$ for $0 \leq x \leq 1$ into $2M_0$ elements of length $\sqrt{2}/(2M_0)$. Thus, the total number of elements is $4M_0$. As in Problem 1, the infinite series in (23), (24), (28), (29) and (31) are truncated by replacing ∞ with the integer N_0 . For selected values of M_0 and N_0 and for a fixed value of v , numerical values of $\phi(x, y)$ are calculated at 5000 randomly selected points in the interior of the solution domains and the average percentage error of the numerical values of ϕ at the 5000 points are shown in Table 2.

Table 2. The average percentage error of $\phi(x, y)$ at 5000 randomly selected points in the solution domain for selected values of v , M_0 and N_0 .

v	$M_0 = 2$ $N_0 = 8$	$M_0 = 5$ $N_0 = 15$	$M_0 = 10$ $N_0 = 30$	$M_0 = 20$ $N_0 = 60$	$M_0 = 40$ $N_0 = 120$
1	0.68%	0.14%	0.06%	0.03%	0.01%
4	1.62%	0.42%	0.16%	0.07%	0.03%
5	5.43%	1.11%	0.32%	0.11%	0.05%

For a fixed value of v , it is obvious that the average percentage error is reduced significantly as the numerical calculation is refined, that is, as M_0 and N_0 increase. For $v = 1$, the average percentage error is less than 1% if 8 boundary elements and 8 terms in the truncated series are used in the calculation. However, it takes 40 elements and 30 terms for $v = 5$ to achieve

the average percentage error of less than 1%. More boundary elements and larger number of terms in the truncated series are required to obtain a better accuracy in calculating the numerical solution for larger values of v . The average percentage error for all selected values of v in Table 2 is less than 0.4% when the total number of elements and the number of terms are more than 40 and 30 respectively. This shows accurate numerical solutions may be obtained for all values of v if sufficient numbers of boundary elements and terms are employed in the numerical calculations.

Problem 3. Consider now solving partial differential equation

$$2\frac{\partial^2\phi}{\partial x^2} + 2\frac{\partial^2\phi}{\partial y^2} - 3\frac{\partial\phi}{\partial x} - 3\frac{\partial\phi}{\partial y} - 20\phi = 0, \quad (37)$$

in the concave region in Figure 1 subject to the boundary conditions

$$\begin{aligned} \phi(x, 0) &= \exp\left(\frac{3}{2}x\right) \text{ for } 0 < x < 1, \\ \phi(x, y) + \frac{\partial\phi(x, y)}{\partial n} &= \frac{4 + 11\sqrt{2}}{4} \exp\left(\frac{3x + 8y}{2}\right) \\ &\text{for } y = 1 - x \text{ and } \frac{1}{2} < x < 1, \\ \phi(x, y) + \frac{\partial\phi(x, y)}{\partial n} &= \frac{4 - 5\sqrt{2}}{4} \exp\left(\frac{3x + 8y}{2}\right) \\ &\text{for } y = x \text{ and } \frac{1}{2} < x < 1, \\ \phi(x, 1) &= \exp\left(\frac{3x + 8}{2}\right) \\ &\text{for } 0 < x < 1, \\ \phi(0, y) + \frac{\partial\phi}{\partial n}\Big|_{x=0} &= -\frac{1}{2} \exp(4y) \\ &\text{for } 0 < y < 1. \end{aligned} \quad (38)$$

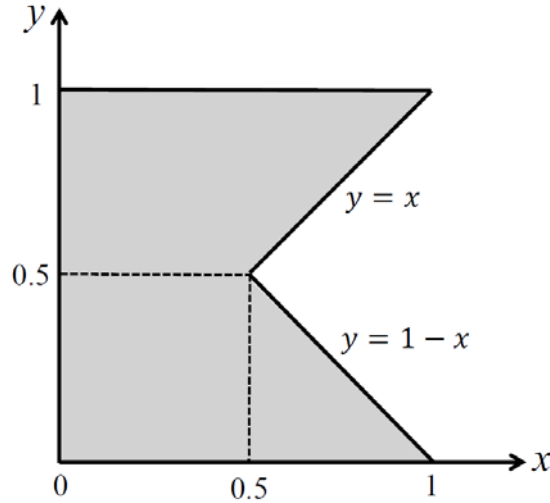


Figure 1. A geometrical sketch for Problem 3.

The analytical solution for the boundary value problem here is given by

$$\phi(x, y) = \exp\left(\frac{3x + 8y}{2}\right).$$

We discretize each of the five sides defining the concave solution domain in Figure 1 into M_0 elements so that $M = 5M_0$ (that is, the total number of boundary elements is $5M_0$). As before, we truncate the infinite series in (23), (24), (28), (29) and (31) by replacing ∞ with the integer N_0 . For selected values of M_0 and N_0 , the complex variable boundary element method is applied to obtain the numerical solutions of $\phi(x, y)$ for the interior points in the solution domain.

Figures 2 and 3 compare graphically the numerical solutions obtained by using three sets of (M_0, N_0) with the corresponding analytical solutions. Figure 2 presents the solutions for $y = 0.9$ and $0 < x < 0.9$ and Figure 3 shows the results for $x = 0.25$ and $0 < y < 1$. As is obvious in the figures, the numerical solution obtained by using the relatively crude approximation $(M_0, N_0) = (4, 15)$ deviates significantly from the corresponding analytical

solution. On the contrary, the solution obtained by using the more refined approximation $(M_0, N_0) = (16, 60)$ agrees well with the analytical solution – the percentage error is less than 1.6%.

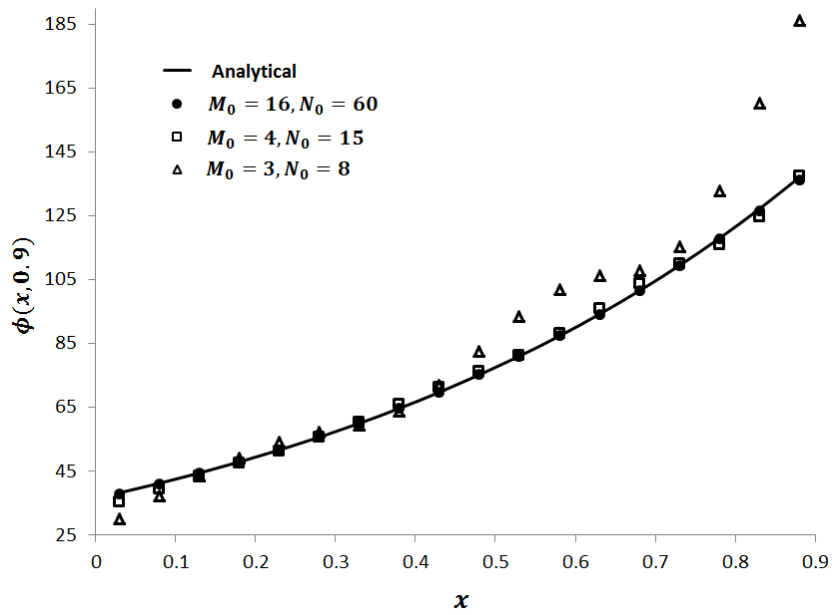


Figure 2. Plots of the numerical and analytical solutions of $\phi(x, 0.9)$ against x .

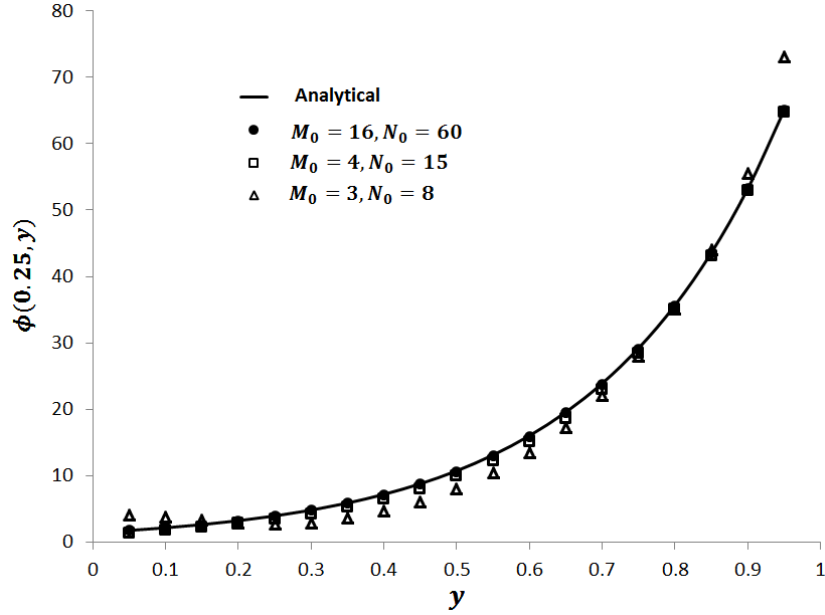


Figure 3. Plots of the numerical and analytical solutions of $\phi(0.25, y)$ against y .

Problem 4. For a practical problem in engineering, we consider here the antiplane deformation of a rectangular slab with a functionally graded shear modulus.

With reference to an $Oxyz$ Cartesian coordinate frame, the slab occupies the region $0 < x < 2$, $0 < y < 1$, $-\infty < z < \infty$. The only non-zero component of the displacement is along the z -axis and is given by $\phi(x, y)$. The corresponding non-zero stress components of interest here are

$$\sigma_{xz} = \sigma_{zx} = \mu \frac{\partial \phi}{\partial x} \text{ and } \sigma_{yz} = \sigma_{zy} = \mu \frac{\partial \phi}{\partial y}, \quad (39)$$

where μ is the shear modulus of the material.

The shear modulus μ of the material in the lab is exponentially graded along the y direction in accordance with

$$\mu = \exp(cy), \quad (40)$$

where c is a given real constant.

Substituting (39) together with (40) into the equilibrium equation of elasticity

$$\frac{\partial \sigma_{xz}}{\partial x} + \frac{\partial \sigma_{yz}}{\partial y} = 0, \quad (41)$$

we obtain the governing partial differential equation

$$\frac{\partial^2 \phi}{\partial x^2} + \frac{\partial^2 \phi}{\partial y^2} + c \frac{\partial \phi}{\partial y} = 0. \quad (42)$$

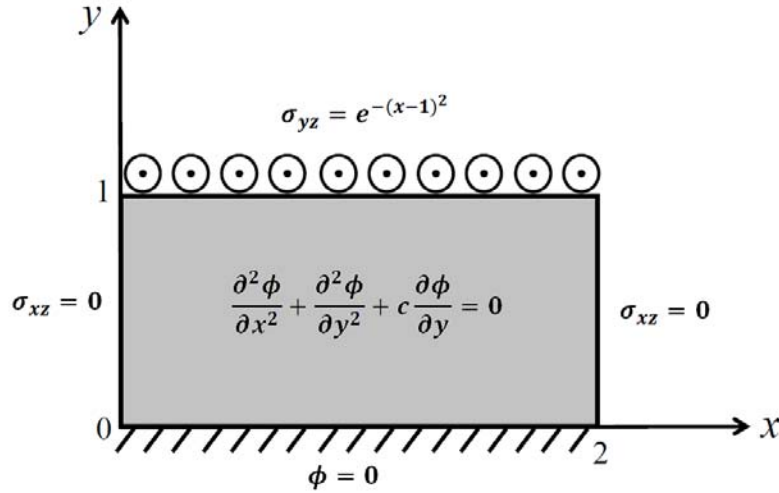


Figure 4. A functionally graded under antiplane deformation.

We are interested in solving (42) subject to

$$\left. \begin{aligned} \phi(x, 0) &= 0 \\ \sigma_{yz}(x, 1) &= e^{-(x-1)^2} \end{aligned} \right\} \text{for } 0 < x < 2, \\ \left. \begin{aligned} \sigma_{xz}(0, y) &= 0 \\ \sigma_{xz}(2, y) &= 0 \end{aligned} \right\} \text{for } 0 < y < 1. \quad (43)$$

The first condition implies that the horizontal side of the slab where $y = 0$ is perfectly attached to a rigid wall, the second condition gives the antiplane traction acting on horizontal side $y = 1$, and the last conditions state that the two vertical sides are traction free. A sketch of the problem is given in Figure 4.

The last three conditions in (43) can be rewritten as

$$\left. \begin{aligned} \left. \frac{\partial \phi}{\partial y} \right|_{y=1} &= e^{-c} e^{-(x-1)^2} \text{ for } 0 < x < 2, \\ \left. \begin{aligned} \left. \frac{\partial \phi}{\partial x} \right|_{x=0} &= 0 \\ \left. \frac{\partial \phi}{\partial x} \right|_{x=2} &= 0 \end{aligned} \right\} \text{for } 0 < y < 1. \end{aligned} \right\} \quad (44)$$

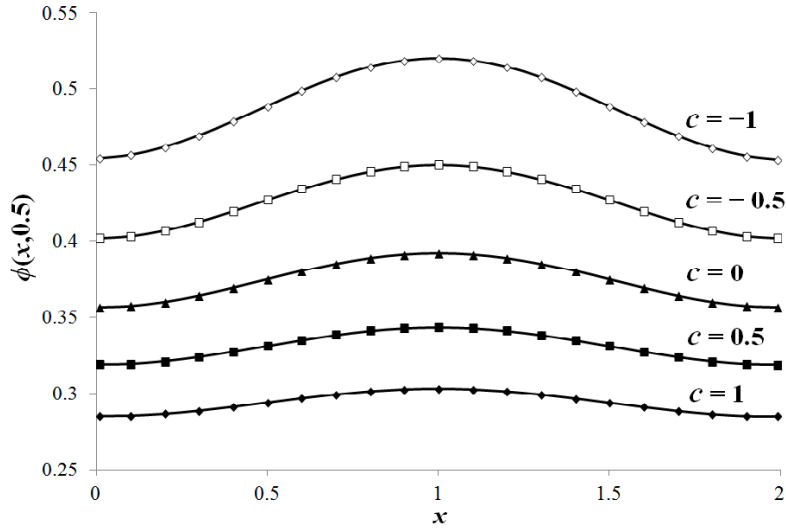


Figure 5. Plots of $\phi(x, 0.5)$ against x for selected values of c .

The complex variable boundary element method is applied to solve (42) in $0 < x < 2$, $0 < y < 1$, subject to the first condition in (43) and the conditions in (44). For selected values of c , the antiplane displacement ϕ on $y = 1/2$ is plotted against x in Figure 5. For a given c , the displacement is largest at $x = 1$. This is to be expected as the load in the second condition in (43) is maximum in magnitude at the point at $x = 1$. As c decreases, the material becomes softer everywhere (except at $y = 0$) and experiences a greater deformation. Thus, in Figure 5, for a fixed x , the displacement increases in magnitude as c decreases from 1 to -1 , as expected.

Problem 5. The complex variable boundary element procedure outlined in Section 3 is for solution domains that are simply connected. Nevertheless, it can be extended to multiply connected solution domains. To show how this may be done, we consider here a problem with a multiply connected solution domain.

The solution domain is as sketched in Figure 6, that is, the exterior boundary of the solution domain are the four sides of the square region $0 < x < 2$, $0 < y < 2$, and the interior boundary is the circle $(x - 3/4)^2 + (y - 3/4)^2 = 1/4$. For a particular boundary value problem, the governing partial differential equation is taken to be

$$\frac{\partial^2 \phi}{\partial x^2} + \frac{\partial^2 \phi}{\partial y^2} - \phi = 0, \quad (45)$$

and we use the particular solution $\phi = e^{-x} + 2e^{-y}$ of (45) to generate boundary data for ϕ on the exterior boundary as well as the interior boundary. If the complex variable boundary element approach outlined below for multiply connected solution domains works, we should be able to use it on the boundary value problem here to recover numerically the solution $\phi = e^{-x} + 2e^{-y}$

at any interior point in the solution domain.

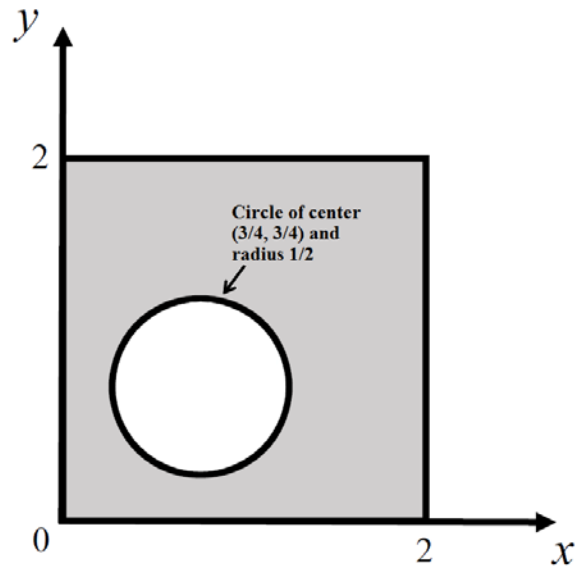


Figure 6. Multiply connected solution domain.

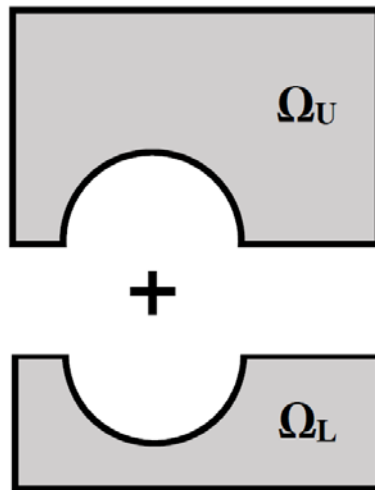


Figure 7. The multiply connected solution domain in Figure 6 is divided into two simply connected subdomains Ω_U and Ω_L .

To solve the boundary value problem, the multiply connected solution domain in Figure 6 is decomposed along the line $y = 3/4$ into two simply connected regions Ω_U and Ω_L as shown in Figure 7. The complex variable boundary element procedure in Section 3 can be modified to construct the required analytic complex function $\Phi_0(z)$ in Ω_U and Ω_L as follows.

Equations (16) and (19), which are obtained by discretizing the first Cauchy integral formula in (12), are still applicable for Ω_U and Ω_L separately. For each of the subdomains Ω_U and Ω_L , the boundary conditions on the parts from the circle and the four sides of the square can be directly expressed as (21) and (26). To link together the two separate complex variable boundary element formulations for Ω_U and Ω_L , we apply continuity conditions involving ϕ and $\partial\phi/\partial n$ along the boundary shared by both Ω_U and Ω_L as given by

$$\left. \begin{aligned} \lim_{\epsilon \rightarrow 0^+} \phi(x, \frac{3}{4} - \epsilon) &= \lim_{\epsilon \rightarrow 0^+} \phi(x, \frac{3}{4} + \epsilon) \\ \lim_{\epsilon \rightarrow 0^+} \frac{\partial\phi}{\partial y} \Big|_{y=3/4-\epsilon} &= \lim_{\epsilon \rightarrow 0^+} \frac{\partial\phi}{\partial y} \Big|_{y=3/4+\epsilon} \end{aligned} \right\}$$

$$\text{for } x \in [0, \frac{1}{4}] \cup [\frac{5}{4}, 2]. \quad (46)$$

The continuity conditions in (46) are approximated in terms of linear algebraic equations in a similar manner as the boundary conditions. Once the linear algebraic equations given by (16), (19), (21) and (26) are solved together with those from (46), the value of ϕ can be computed at any point in the interior of the solution domain using (31) corresponding to Ω_U or Ω_L depending on whether the interior point lies in Ω_U or Ω_L .

Table 3. A comparison of the numerical and analytical solutions at selected interior points of the solution domain.

Point (x, y)	Numerical solution	Analytical solution
(0.1, 0.1)	2.72405	2.71451
(0.1, 0.2)	2.55097	2.54230
(0.1, 0.3)	2.39462	2.38647
(0.1, 0.5)	2.12596	2.11790
(0.1, 0.7)	1.90214	1.89801
(0.1, 0.9)	1.71664	1.71798
(0.1, 1.1)	1.57058	1.57058
(0.1, 1.3)	1.45017	1.44990
(0.1, 1.5)	1.35140	1.35110
(0.1, 1.9)	1.20492	1.20397
(0.5, 0.1)	2.42311	2.41621
(0.5, 0.2)	2.25680	2.24399
(0.5, 1.3)	1.15186	1.15159
(0.5, 1.5)	1.05308	1.05279
(0.5, 1.9)	0.90591	0.90567
(1.0, 0.1)	2.17740	2.17755
(1.0, 0.2)	2.00203	2.00534
(1.0, 1.3)	0.91396	0.91294
(1.0, 1.5)	0.81552	0.81414
(1.0, 1.0)	0.66709	0.66701
(1.5, 0.1)	2.03276	2.03280
(1.5, 0.2)	1.86339	1.86059
(1.5, 0.3)	1.71140	1.70477
(1.5, 0.5)	1.45585	1.43619
(1.5, 0.7)	1.26391	1.21630
(1.5, 0.9)	1.07357	1.03627
(1.5, 1.1)	0.90671	0.88887
(1.5, 1.3)	0.77720	0.76819
(1.5, 1.5)	0.67398	0.66939
(1.5, 1.9)	0.52237	0.52227
Average % error	0.45%	–

The numerical values of ϕ at interior points throughout the solution domain, obtained using a total of 104 boundary elements, are compared with the analytical solution in Table 3. The numerical and analytical solutions agree well with each other. The average percentage difference between the solutions is less than 0.5%. This indicates that the complex variable boundary element procedure can be readily extended to multiply connected solution domains by using the approach described above.

5 Summary

A complex variable boundary element method is proposed here for solving numerically a two-dimensional boundary value problem governed by a steady-state advection-diffusion-reaction equation. The solution of the advection-diffusion-reaction equation is formulated in terms of a single complex function which is holomorphic in the solution domain. The Cauchy integral formula and its differentiated form are used together with the boundary conditions of the boundary value problem to construct approximately the required complex function. This gives rise to a system of linear algebraic equations. The numerical procedure requires only the boundary of the solution domain to be discretized into straight line elements. Once the complex function is constructed, the solution of the boundary value problem can be computed numerically at any point in the interior of the solution domain.

To test the validity and accuracy of the proposed complex variable boundary element method, it (the method) is applied to solve numerically some specific boundary value problems. The numerical solutions for all the test problems show convergence to the analytical solutions when the calculations are properly refined. This indicates that the proposed complex variable bound-

ary element method is correctly formulated and can be employed as a useful alternative numerical method for solving boundary value problems governed by the steady-state two-dimensional advection-diffusion-reaction equation. For a problem of practical interest in engineering, the method is applied to analyze the antiplane deformation of a functionally graded slab. It is also successfully extended to solve a boundary value problem involving a multiply connected solution domain.

Acknowledgment

The authors would like to thank an anonymous reviewer for giving constructive feedback on the research work here as well as for suggesting to solve a boundary value problem involving a multiply connected solution domain.

References

- [1] W. T. Ang, A note on the CVBEM for the Helmholtz equation or its modified form, *Communications in Numerical Methods in Engineering* **18** (2002) 599-604.
- [2] W. T. Ang, The two-dimensional reaction-diffusion Brusselator system: A dual-reciprocity boundary element solution. *Engineering Analysis with Boundary Elements* **27** (2003) 897-903.
- [3] Ang WT and Park YS, CVBEM for a system of second order elliptic partial differential equations, *Engineering Analysis with Boundary Elements* **21** (1998) 197-184.

- [4] G. Barone, A. Pirrotta and R. Santoro, Comparison among three boundary element methods for torsion problems: CPM, CVBEM, LEM, *Engineering Analysis with Boundary Elements* **35** (2011) 895-907.
- [5] G. Barone and A. Pirrotta, CVBEM for solving De Saint-Venant solid under shear forces, *Engineering Analysis with Boundary Elements* **37** (2013) 197-204.
- [6] J. T. Chen and Y. W. Chen, Dual boundary element analysis using complex variables for potential problems with or without a degenerate boundary, *Engineering Analysis with Boundary Elements* **24** (2000) 671-684.
- [7] D. L. Clements and C. Rogers, A boundary integral equation method for the solution of a class of problems in anisotropic inhomogeneous thermostatics and elastostatics, *Quarterly of Applied Mathematics* **41** (1983) 99-105.
- [8] W. Dai and R. Nassar, A finite difference scheme for the generalized nonlinear Schrodinger equation with variable coefficients, *Journal of Computational Mathematics* **18** (2000) 123-132.
- [9] A. B. Gumel, W. T. Ang and E. H. Twizell, Efficient parallel algorithm for the two-dimensional diffusion equation subject to specification of mass, *International Journal of Computer Mathematics* **64** (1997) 153-163.
- [10] T. V. Hromadka and C. Lai, *The Complex Variable Boundary Element Method in Engineering Analysis*, Springer-Verlag, Berlin, 1987.

- [11] B. Q. Li and J. W. Evans, Boundary element solution of heat convection-diffusion problems, *Journal of Computational Physics* **93** (1991) 225-272.
- [12] A. M. Linkov and S. G. Mogilevskaya, Complex hypersingular integrals and integral equations in plane elasticity, *Acta Mechanica* **105** (1994) 189-205.
- [13] Y. S. Park and W. T. Ang, A complex variable boundary element method for an elliptic partial differential equation with variable coefficients, *Communications in Numerical Methods in Engineering* **16** (2000) 697-703.
- [14] K. Sato, Complex variable boundary element method for potential flow with thin objects, *Computer Methods in Applied Mechanics and Engineering* **192** (2003) 1421-1433.
- [15] K. M. Singh and M. Tanaka, On exponential variable transformation based boundary element formulation for advection-diffusion problems, *Engineering Analysis with Boundary Elements* **24** (2000) 225-236.
- [16] M. Skote, Scaling of the velocity profile in strongly drag reduced turbulent flows over an oscillating wall, *International Journal of Heat and Fluid Flow* **50** (2014) 352-358.

Appendix

As in Ang [1], the functions $h_m(x)$ in (3) or (9) can be obtained by letting

$$h_m(x) = h_0(x) \sum_{r=0}^m \beta_m^{(r)} x^r, \quad (\text{A1})$$

where $\beta_0^{(0)} = 1$ and $\beta_m^{(r)}$ ($r = 0, 1, 2, \dots, m$) (for any given $m > 0$) are constants (possibly complex) yet to be determined.

Substituting (A1) into (7) and collecting like powers of x , we find that, for any given $m > 0$,

$$\beta_m^{(0)} = 0, \quad (\text{A2})$$

$$2\lambda\beta_m^{(r)} = -\frac{\lambda(r+1)\beta_{m-1}^{(r+1)}}{m} - \frac{iv\beta_{m-1}^{(r)}}{m} + \frac{1}{mr} \left(\frac{u^2 + v^2}{4\lambda} + k \right) \beta_{m-1}^{(r-1)} \text{ for } r = 1, 2, \dots, m-2, \quad (\text{A3})$$

$$2\lambda\beta_m^{(m-1)} = -\frac{iv\beta_{m-1}^{(m-1)}}{m} + \frac{1}{(m-1)m} \left(\frac{u^2 + v^2}{4\lambda} + k \right) \beta_{m-1}^{(m-2)}, \quad (\text{A4})$$

and

$$2\lambda\beta_m^{(m)} = \frac{1}{m^2} \left(\frac{u^2 + v^2}{4\lambda} + k \right) \beta_{m-1}^{(m-1)}. \quad (\text{A5})$$